

## Design, preparation and characterization of a novel BiFeO<sub>3</sub>/CuWO<sub>4</sub> heterojunction catalyst for one-pot synthesis of trisubstituted imidazoles

Hamed Ramezanalizadeh

Young Researchers and Elites Club, Roodsar Branch, Islamic Azad University, Roodsar, Iran

Received: 26 November 2016, Accepted: 5 April 2017, Published: 5 April 2017

### Abstract

In this work, a novel heterojunction catalyst has been synthesized and employed as a highly efficient catalyst for one-pot synthesis of substituted imidazoles. Analytical methods including Fourier transform infrared (FT-IR), diffuse reflectance spectroscopy (DRS), X-ray diffraction (XRD), Energy-dispersive X-ray spectroscopy (EDX), Scanning electron microscopy (SEM) and Vibrating Sample Magnetometer (VSM) were used for the catalyst characterization. Moreover, the catalyst was also recovered and reused five times without remarkable decrease in its catalytic activity. Compared to the classical methodologies, this method illustrated significant advantages including low loading of the catalyst, short reaction times, high to excellent yields, easy separation and purification of the products.

**Keywords:** BiFeO<sub>3</sub>/CuWO<sub>4</sub>; heterogeneous catalyst; trisubstituted imidazoles; solvent free; magnetic BiFeO<sub>3</sub>.

### Introduction

During the last decade, multiferroic materials attracted considerable attention due to their technological and fundamental importance [1]. Perovskite-type oxides with the general elemental composition of ABO<sub>3</sub>, where A is a rare earth metal and B a transition metal, have attracted many scientists due to their fascinating and well defined structure and intrinsic properties. Perovskite compounds have numerous applications such as multiferroic, photocatalytic, and magnetic properties which are useful for applications in nonlinear optics, photoelectrochemical cell, thin-film capacitor, catalysts, and nonvolatile memory [2].

Among the multiferroic materials studied so far, BiFeO<sub>3</sub> (BFO) is perhaps the only one that exhibits both ferroelectricity and G-type antiferromagnetism [3]. Recently a perovskite-type BiFeO<sub>3</sub> photocatalyst (BFO) has attracted considerable attention owing to the narrow band-gap energy (2.1eV)[4], and high chemical stability in addition to acting as a well-known multiferroic compound, exhibiting a coexistence of simultaneous ferroelectric and magnetic order parameters [5,6]. However, due to its low surface area and high ratio recombination of electron/hole pairs, it needs to be combined with foreign materials that could offer a high surface area with electron transport ability [7,8]. For instance Dai combined

\*Corresponding author: Hamed Ramezanalizadeh  
Tel: +98 (21) 66298742, Fax: +98 (21) 66086717  
E-mail: hramzanalizadeh@gmail.com

BiFeO<sub>3</sub> with garphene significantly enhanced the photocatalytic activity for the MO degradation [9]. Various methods have been developed for the preparation of micrometer and nanometer-sized BiFeO<sub>3</sub> crystallites, such as Co-precipitation [10,11], sol-gel process [12,13], hydrothermal route [14,15], conventional solid state reaction [16,17] and thermal decomposition route [18]. In addition to potential electronic applications, BFO have been used as a new visible-light photocatalyst [19] and a vector in drug targeting to minimize the side effects of drugs in chemotherapy [20].

Despite the fact that some work in this area has been undertaken, various research avenues such as synthesis, characterization and the catalytic properties are yet to be explored. Orthotungstates are technologically important materials with special prominence in their use as scintillation detectors, lasers, photoanodes, and optical fibers [21]. Copper tungstate (CuWO<sub>4</sub>) is a well-known n-type semiconductor which has attracted increasing interest due to these applications [22]. Copper tungstate (CuWO<sub>4</sub>) is belonging to the family of structurally related divalent transition metal tungstates. These compounds contain 3d orbital corresponding to the transition metals which are responsible for the electronic correlation effects observed in these materials [23].

Development of new multicomponent reactions (MCRS) are an area of considerable interest due to the fact that the products are formed in a single step and also a variety could be achieved only by changing the reaction components [24].

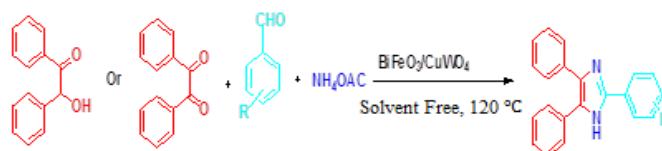
Imidazole derivatives are a very interesting class of heterocyclic compounds because they have many pharmacological properties and play

important roles in biological process. The imidazole compounds are known to possess NO synthase inhibition and antifungal, antimycotic, antitumor, antibiotic, antibacterial, antiulcerative, and CB1 receptor antagonistic activities [25,26]. Various substituted imidazoles act as B-Raf kinase [27], glucagon receptors [28], inhibitors of p38 MAP kinase [29], plant grown regulators [30], therapeutic agents [31] and pesticides [32,33]. These propellants have engendered considerable interest among synthetic organic and medicinal chemists in recent years. Accordingly, a number of synthetic methods have been reported for the synthesis of 2,4,5-trisubstituted imidazoles. These methods involve condensation of benzil or benzoin, aryl aldehydes and ammonium acetate using various catalytic systems [34-38]. But, some of these synthetic methods are associated with one or more drawbacks such as using expensive reagents, long reaction times, purifications, complex work-up, generation of large amount of toxic wastes, strongly acidic conditions, high temperature, poor yields and occurrence of side reactions.

Owing to the wide range of pharmacological and biological activities, the development of effective, high yielding, economical, clean and mild environmental benign protocols is still desirable and is in demand. Moreover, the design of valuable, effective and recoverable catalysts is important for the both environmental and economical point of view. Herein we wish to report a new efficient and practical route for the synthesis of trisubstituted imidazoles by the condensation reaction of benzil or benzoin, aryle aldehydes and ammonium acetate that catalyzed by novel BiFeO<sub>3</sub>/CuWO<sub>4</sub> heterojunction particles. To the best of our knowledge,

this is the first report of design, preparation, and characterization of BiFeO<sub>3</sub>/CuWO<sub>4</sub> heterojunction and its application as a heterogeneous catalyst in organic reactions. This novel approach has several superiorities compared to the previous reports for the synthesis of substituted imidazole

derivatives and opens an important area to the use of environmentally benign and recoverable heterogeneous nanocatalyst in the synthesis of pharmaceutically important heterocyclic compounds (Scheme 1).



**Scheme 1.** One-pot synthesis of trisubstituted imidazoles catalyzed by BiFeO<sub>3</sub>/CuWO<sub>4</sub>

## Experimental

### General

In this study, all reagents and starting materials were obtained commercially from Sigma-Aldrich and Merck, and were used as received without any further purification unless otherwise noted. FT-IR analyses were carried out on a Shimadzu FTIR-8400S spectrophotometer using a KBr pallet for sample preparation. X-ray powder diffraction (XRD) patterns were recorded using a Cu radiation ( $\lambda=1.5406$ ) source on a STOE powder diffraction system. The morphologies of the prepared catalyst was observed by an AIS2100 (Seron Technology) scanning electron microscopy (SEM). DRS spectra was prepared via a Shimadzu (MPC-2200) spectrophotometer. A commercial HH-15 model vibrating sample magnetometer (VSM, Lakeshore 7410) was used at room temperature to characterize the magnetic properties of BiFeO<sub>3</sub> and BiFeO<sub>3</sub>/CuWO<sub>4</sub> particles. <sup>1</sup>H and <sup>13</sup>C spectra were recorded on a Bruker DRX-400 Avance spectrometer at 400 and 100 MHz. Atomic Absorption spectroscopy (AAS) was carried out on a PinAAcle 900F instrument model.

### General procedure for the synthesis of 2,4,5-trisubstituted -1H-imidazoles

BiFeO<sub>3</sub>/CuWO<sub>4</sub> as a highly efficient magnetic catalyst was added to a mixture of benzil or benzoin, benzaldehyde (1mmol) and NH<sub>4</sub>OAc. The resulting mixture was heated at 120 °C (bath temperature) under mild solvent-free conditions. After the completion of the reaction, as indicated by TLC, the reaction was cooled to room temperature. The resultant solid was dissolved in acetone and the magnetic catalyst was separated using an external magnet. After catalyst separation, the filtered solution retained a product, which was placed in the refrigerator to obtain pure crystalline products in good-to-high yields.

### Preparation of catalyst

#### Synthesis of BiFeO<sub>3</sub>

BiFeO<sub>3</sub> was synthesized according to a modified sol-gel method [39]. A transparent multi-component solution was prepared by mixing bismuth and iron salts. Bismuth nitrate pentahydrate, Bi(NO<sub>3</sub>)<sub>3</sub>·5H<sub>2</sub>O was dissolved at room temperature in a mixture of 2-methoxyethanol and acetic acid. Then it was mixed with equimolar amount of iron nitrate to obtain the BiFeO<sub>3</sub> xerogel powder. The precursor solution

was dried at 80 °C for about 12 h to obtain the BiFeO<sub>3</sub> xerogel powder. Then xerogel powder was ground and the powder annealed at 600 °C for 30 min in air or N<sub>2</sub> atmosphere in furnace. During the annealing procedure, heating and cooling rates of furnace were maintained at a rate of 4 °C/min.

### Synthesis of BiFeO<sub>3</sub>/CuWO<sub>4</sub> Composite

The BiFeO<sub>3</sub>/CuWO<sub>4</sub> heterojunction catalyst was prepared through an impregnation process. The above-obtained BiFeO<sub>3</sub> powder with the predetermined amount was impregnated in an aqueous solution containing a given amount of Cu(NO<sub>3</sub>)<sub>2</sub>.3H<sub>2</sub>O and Na<sub>2</sub>WO<sub>4</sub>.2H<sub>2</sub>O. The suspension was sonicated for 2 h to make it homogeneous and then was continuously stirred till the water was totally evaporated on a water bath at 70 °C. Afterwards, the dried powder was ground and annealed in a furnace at 600 °C for 2 h to decompose the Cu(NO<sub>3</sub>)<sub>2</sub>.3H<sub>2</sub>O and Na<sub>2</sub>WO<sub>4</sub>.2H<sub>2</sub>O to CuWO<sub>4</sub> which were in close contact with BiFeO<sub>3</sub> powder.

### Results and discussion

In this work we synthesized a heterostructure composite system containing BiFeO<sub>3</sub> and CuWO<sub>4</sub> mixed metal oxides. After synthesis, we used heterostructure as a highly efficient and novel catalyst for the one-pot synthesis of substituted imidazoles under mild solvent-free conditions. In order to confirm the BiFeO<sub>3</sub>/CuWO<sub>4</sub> heterostructure composite system we employed different characterization techniques such as X-ray powder diffraction (XRD), Fourier transform

infrared spectroscopy (FT-IR), Diffuse reflectance spectroscopy (DRS), Scanning electron spectroscopy (SEM), Energy dispersive x-ray spectroscopy (EDS) and Vibrating Sample Magnetometry (VSM). The XRD patterns of five materials including BiFeO<sub>3</sub>/CuWO<sub>4</sub>, synthesized BiFeO<sub>3</sub>, simulated BiFeO<sub>3</sub>, synthesized CuWO<sub>4</sub> and simulated CuWO<sub>4</sub> are shown in (Figure 1a-e), respectively. All the diffraction peaks in the synthesized BiFeO<sub>3</sub> pattern (Figure 1b) are indexed as the pure BiFeO<sub>3</sub> structure (Figure 1c). The diffraction peaks of pure BiFeO<sub>3</sub> sample is in good agreement with pure rhombohedral phase of BiFeO<sub>3</sub> (JCPDS No. 2-169) shown in (Figure 1b,c). There are no impure peaks found, suggesting the high purity and crystallinity of the sample. Powder x-ray diffraction compares the simulated and experimental x-ray diffraction patterns (Figure 1). All the diffraction peaks in CuWO<sub>4</sub> XRD pattern are indexed as the triclinic CuWO<sub>4</sub> structure (Figure 1d). According to JCPDS card numbers the peaks at 2 $\theta$  values of 18.1<sup>o</sup>, 19.0<sup>o</sup>, 22.9<sup>o</sup>, 23.5<sup>o</sup>, 24.1<sup>o</sup>, 25.9<sup>o</sup>, 26.9<sup>o</sup>, 28.7<sup>o</sup>, 30.1<sup>o</sup>, 30.8<sup>o</sup>, 31.6<sup>o</sup>, 32.1<sup>o</sup>, 34.4<sup>o</sup> and 38.6<sup>o</sup> can be indexed to (0,0,1), (1,0,0), (1,1,0), (0,-1,1), (0,1,1), (-1,0,1), (1,0,1), (-1,-1,1), (1,1,1), (0,2,0), (-1,1,1), (1,-1,1), (1,2,0) and (2,0,0) crystal planes, respectively. No other impurity peaks were detected, indicating the high crystallinity level of CuWO<sub>4</sub> structure. Furthermore, for the BiFeO<sub>3</sub>/CuWO<sub>4</sub> product, the XRD pattern of (Figure 1a) matches well with those of BiFeO<sub>3</sub> and CuWO<sub>4</sub> phases in the composite.

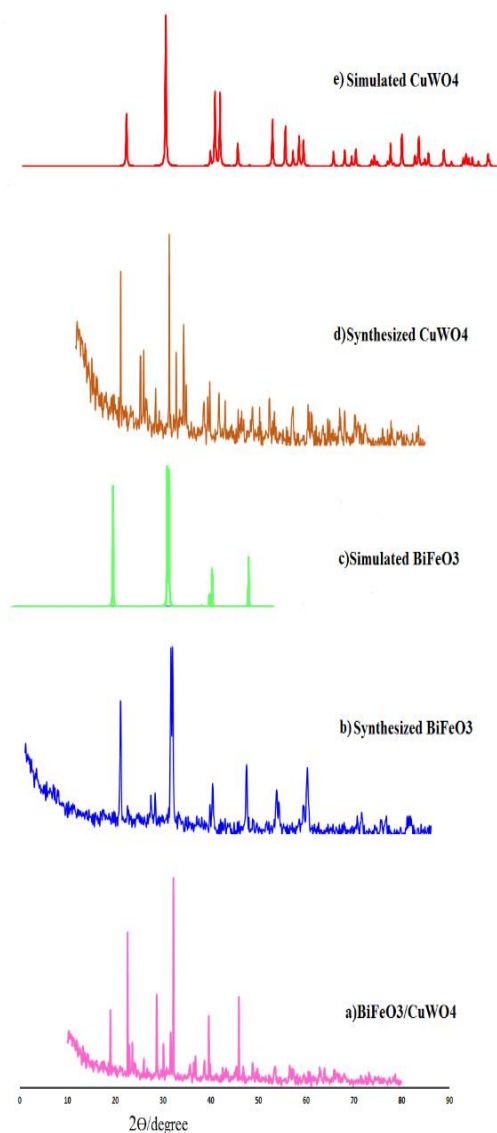


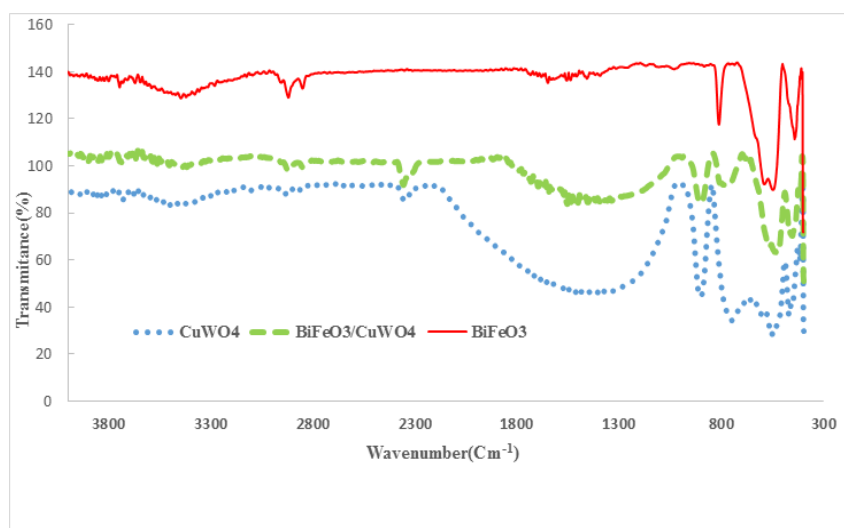
**Figure 1.** PXRD patterns of a) BiFeO<sub>3</sub>/CuWO<sub>4</sub>, b) Synthesized BiFeO<sub>3</sub>, c) Simulated BiFeO<sub>3</sub>, d) Synthesized CuWO<sub>4</sub> and e) Simulated CuWO<sub>4</sub>

FT-IR spectrum of BiFeO<sub>3</sub>, CuWO<sub>4</sub> and BiFeO<sub>3</sub>/CuWO<sub>4</sub> structures have also been investigated and shown in Figure 2. In the FT-IR spectrum of BiFeO<sub>3</sub> shown in Figure 2. The broad band around 3442.5 cm<sup>-1</sup> arises from the antisymmetric and symmetric vibration bands of H<sub>2</sub>O and OH groups. Specifically, two strong absorptive peaks around 545.8 and 441.7 cm<sup>-1</sup> are attributed to the Fe–O stretching and O–Fe–O bending

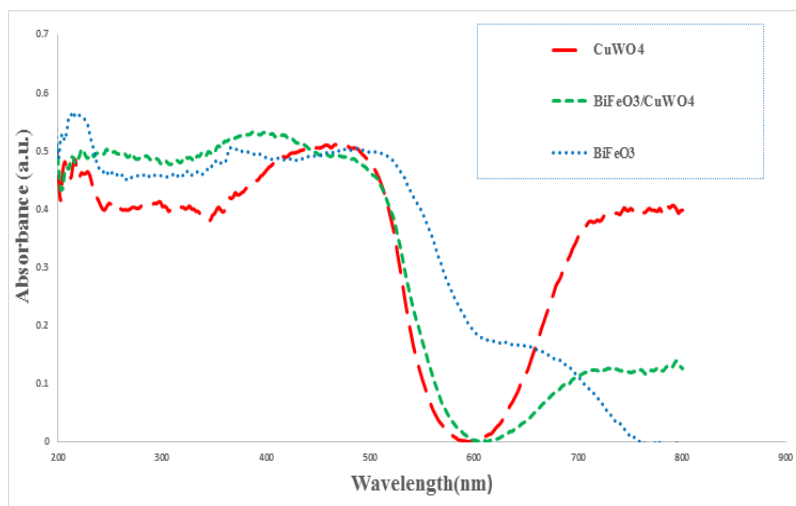
vibrations, being characteristics of the octahedral FeO<sub>6</sub> groups in the perovskite compounds. The formation of perovskite structure can be confirmed by the presence of metal-oxygen band [40]. In the CuWO<sub>4</sub> FT-IR spectrum the bands which appear at a lower frequency are assigned to the deformation modes of the WO<sub>4</sub> tetrahedra. The absorption bands that appear in the 901 cm<sup>-1</sup> assigned to stretching mode of W–O bonds in

junction with  $\text{WO}_4$  tetrahedra. Furthermore, the bands appearing in the  $760\text{ cm}^{-1}$  are due to the Cu-O stretching band. The appearing absorption bands below  $600\text{ cm}^{-1}$  might be related to the deformation modes of W-O bonds in the  $\text{WO}_4$  tetrahedra or the deformation modes of W-O-W bridges. Presence of several splitting absorption peaks at  $569$ ,  $585$ ,  $774$  and  $902\text{ cm}^{-1}$  can be attributed to the  $\text{CuWO}_4$  phase. Furthermore, annealing of the sample at higher temperatures ( $600\text{ }^\circ\text{C}$ ) creates stronger W-O bonds due to the improvement of the sample crystallinity. As illustrated in the FT-IR spectrum of the  $\text{BiFeO}_3/\text{CuWO}_4$

(Figure 2.) separate and common absorption peaks of  $\text{BiFeO}_3$  and  $\text{CuWO}_4$  can be seen with the composite formation. Diffuse reflectance spectroscopy of pure  $\text{BiFeO}_3$ ,  $\text{CuWO}_4$  and  $\text{BiFeO}_3/\text{CuWO}_4$  heterostructure composite samples are illustrated in Figure 3. As can be seen  $\text{BiFeO}_3$  displays absorbance in the shorter wavelength region compared with the composite, while the DRS of  $\text{BiFeO}_3/\text{CuWO}_4$  have red shift in the absorption that revealed the presence of  $\text{CuWO}_4$  added to the  $\text{BiFeO}_3$  which could shift its optical absorbance edge into more visible light range.



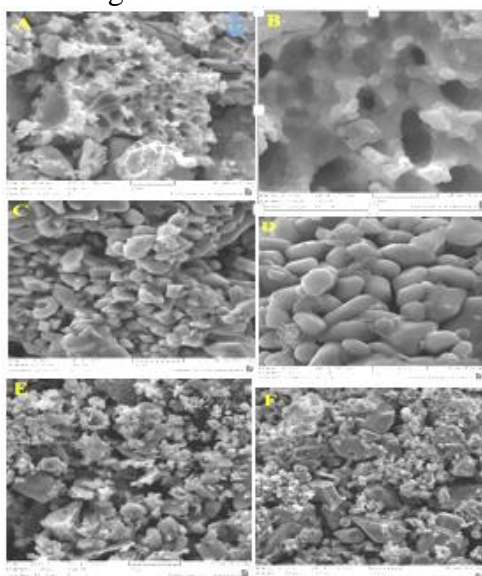
**Figure 2.** The FT-IR spectra of pure  $\text{BiFeO}_3$ ,  $\text{BiFeO}_3/\text{CuWO}_4$  heterojunction and  $\text{CuWO}_4$



**Figure 3.** The DRS spectra of pure  $\text{CuWO}_4$ ,  $\text{BiFeO}_3/\text{CuWO}_4$  heterojunction and  $\text{BiFeO}_3$

Scanning electron microscopy (SEM) images were taken to directly analyse the morphology of the prepared samples. The SEM images of as-prepared pure  $\text{BiFeO}_3$ ,  $\text{CuWO}_4$  and  $\text{BiFeO}_3/\text{CuWO}_4$  heterojunctions are given in (Figure 4.). A typical SEM images of pure  $\text{BiFeO}_3$  is shown in (Figure 4a,b). The samples are wafer-like morphology that also shows high poros structure. SEM images of

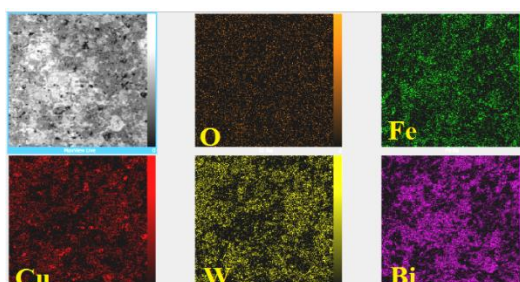
$\text{CuWO}_4$  have also been investigated and shown in (Figure 4 c,d). According to the SEM images,  $\text{CuWO}_4$  belonging grain-like structure with the uniform morphology. SEM images of  $\text{BiFeO}_3/\text{CuWO}_4$  heterostructure composite obviously shows the interface of  $\text{BiFeO}_3$  and  $\text{CuWO}_4$  structure. Furthermore, the composition of magnetic  $\text{BiFeO}_3$  and  $\text{CuWO}_4$  can be seen.



**Figure 4.** The SEM images of pure  $\text{BiFeO}_3$  (top), pure  $\text{CuWO}_4$  (middle) and  $\text{BiFeO}_3/\text{CuWO}_4$  (bottom)

The energy dispersive X-ray spectroscopy (EDX) was used to determine the presence of elements in the  $\text{BiFeO}_3/\text{CuWO}_4$  heterojunction. EDX elemental mapping images revealed that Bi, Fe, O, Cu and W components were distributed uniformly

on the  $\text{BiFeO}_3/\text{CuWO}_4$  structure (Figure 5). The EDX spectrum of Figure 5 was taken on the surface structure illustrates composition as O, Fe, Cu, W and Bi elements with the weight ratio of 27.72, 2.46, 7.32, 21.12 and 41.39, respectively.



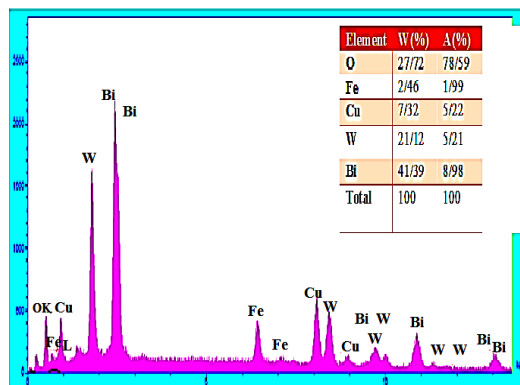


**Figure 5.** EDX elemental mapping images of the  $\text{BiFeO}_3/\text{CuWO}_4$  for Bi, Fe, O, Cu, W elements and percentage of elements in  $\text{BiFeO}_3/\text{CuWO}_4$  heterostructure composite

To investigate the magnetic properties of  $\text{BiFeO}_3$  and  $\text{BiFeO}_3/\text{CuWO}_4$  the hysteresis loops were measured by VSM at room temperature. Figure 5 shows their magnetization curves. Zero coercivity for both samples were obtained, which indicates that the saturation magnetization value ( $M_s$ ) for

bare  $\text{BiFeO}_3$  and  $\text{BiFeO}_3/\text{CuWO}_4$  is 65.9 and 56.23 emu/g, respectively. In other words, with the presence of  $\text{CuWO}_4$  the magnetic saturation decreased slightly. The magnetic loop follows almost linear field-dependence of magnetization.

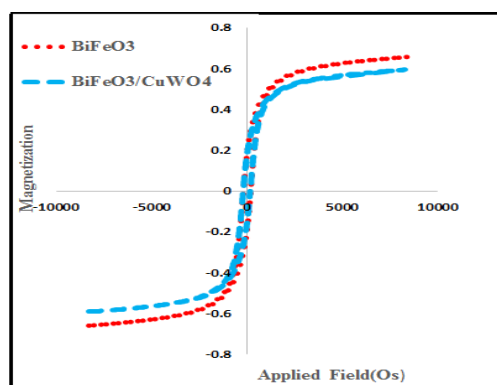


**Figure 6.** Magnetization curves obtained by VSM at room temperature for  $\text{BiFeO}_3$  and  $\text{BiFeO}_3/\text{CuWO}_4$  heterojunction

To put in evidence the role and effect of catalyst in rate of reaction, the model reaction was carried out in the absence of any catalyst (Table 1, Entry 1). The results revealed that yield of reaction was very low, and the time has not had remarkable impact on the efficiency of reaction. To evaluate the

convenient catalyst loading, the model reaction was carried out using different amounts of catalyst. It was found that the most suitable amount of catalyst is 15 mg (Table 1, Entry 8) and larger amount of catalyst do not increase the reaction yield.



**Table 1.** Optimization of reaction conditions catalysed by BiFeO<sub>3</sub>/CuWO<sub>4</sub> heterojunction

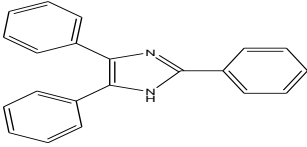
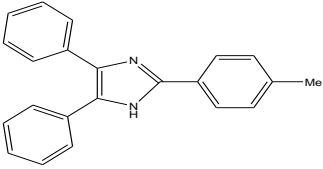
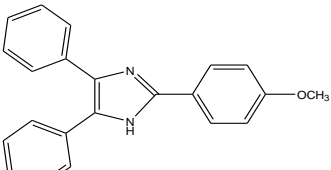
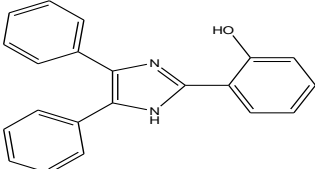
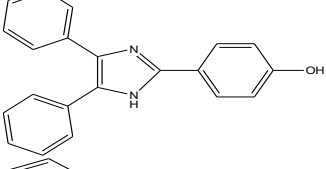
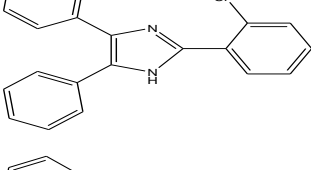
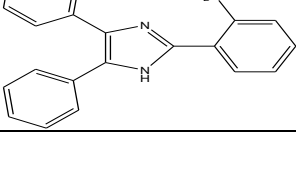
Entry	Catalyst(mg)	Condition	Temperature( <sup>0</sup> C)	Time(min) <sup>a</sup>	Yield(%) <sup>b</sup>
1	0	Solvent free	80	30	0
2	1	Solvent free	100	30	10
3	5	Solvent free	120	30	10
4	8	Solvent free	120	30	50
5	10	Solvent free	120	30	70
6	12	Solvent free	120	30	75
7	15	Solvent free	25	60	30
8	15	Solvent free	120	10	95
9	15	Solvent free	130	35	87
10	15	Solvent free	150	35	75
11	15	EtOH	Reflux	60	86
12	15	H <sub>2</sub> O	Reflux	60	30
13	15	CH <sub>3</sub> CN	Reflux	60	5
14	15	THF	Refl	125	31

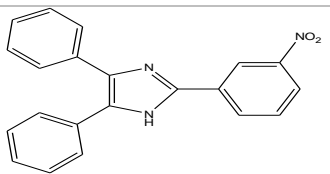
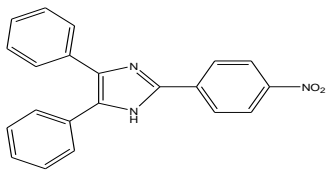
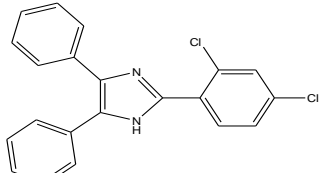
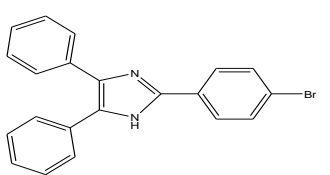
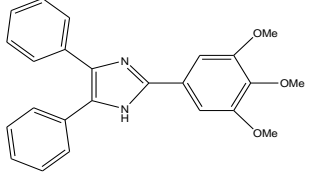
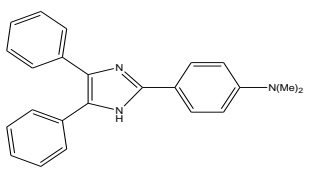
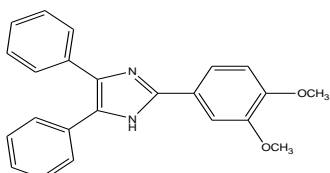
Experimental condition: Benzil (1 mmol), 3-Nitrobenzaldehyde (1mmol) and ammonium acetate (2.5mmol)

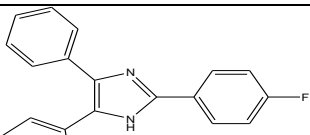
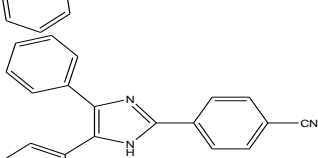
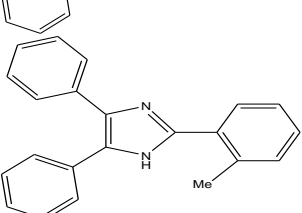
<sup>a</sup>Reaction progress monitored by TLC.

<sup>b</sup>Isolated Yield.

**Table 2.** Synthesis of 2,4,5-trisubstituted-1H-imidazoles using BiFeO<sub>3</sub>/CuWO<sub>4</sub> catalyst under solvent-free conditions

Entry	Product	Time (min)		Yield (%) <sup>a</sup>		Mp (°C)	Lit. MP(°C) (Ref)
		Benzil	Benzoin	Benzil	Benzoin		
1		10	14	95	93	270-271	272-274 (Ref.40)
2		10	15	94	90	228-230	230-232 (Ref.41)
3		15	20	90	86	227-229	228-231 (Ref. 40)
4		12	16	92	85	203-205	203-205 (Ref.42)
5		15	20	95	92	230-232	227-229 (Ref.43)
6		20	25	94	91	190-192	190-191 (Ref. 44)
7		15	25	87	85	230-231	230-232 (Ref. 45)

<b>8</b>		7	15	95	93	290-291	297-299 (Ref. 44)
<b>9</b>		8	10	94	91	199-201	299-201 (Ref. 46)
<b>10</b>		10	15	98	93	177-178	173-174 (Ref. 47)
<b>11</b>		12	20	94	92	261-263	261-263 (Ref. 42)
<b>12</b>		15	20	95	91	262-263	261-262 (Ref. 48)
<b>13</b>		15	30	89	84	260-261	260-261 (Ref. 49)
<b>14</b>		20	25	95	92	216-218	213-215 (Ref. 48)

15		17	21	85	81	196-198	196-198 (Ref. 43)
16		10	15	95	92	234-236	236-237 (Ref. 50)
17		15	25	87	81	203-205	205-207 (Ref. 51)

<sup>a</sup>Yields refer to isolated pure products. The known products were characterized and compared by their physical properties with authentic samples.

After optimizing the reaction conditions, and in order to investigate the efficiency and applicability of this catalyst in the synthesis of 2,4,5-1H-imidazoles the reaction was extended to other substituted benzaldehydes at 120 °C in solvent-free conditions. It is obvious from Table 2 that when benzoin was used instead of benzil the reaction time increased. These results show that all the aromatic aldehydes having either electron-withdrawing substituted and electron-donating ones demonstrate excellent reactivity and yields to afford corresponding substituted 2,4,5-1H-imidazole derivatives.

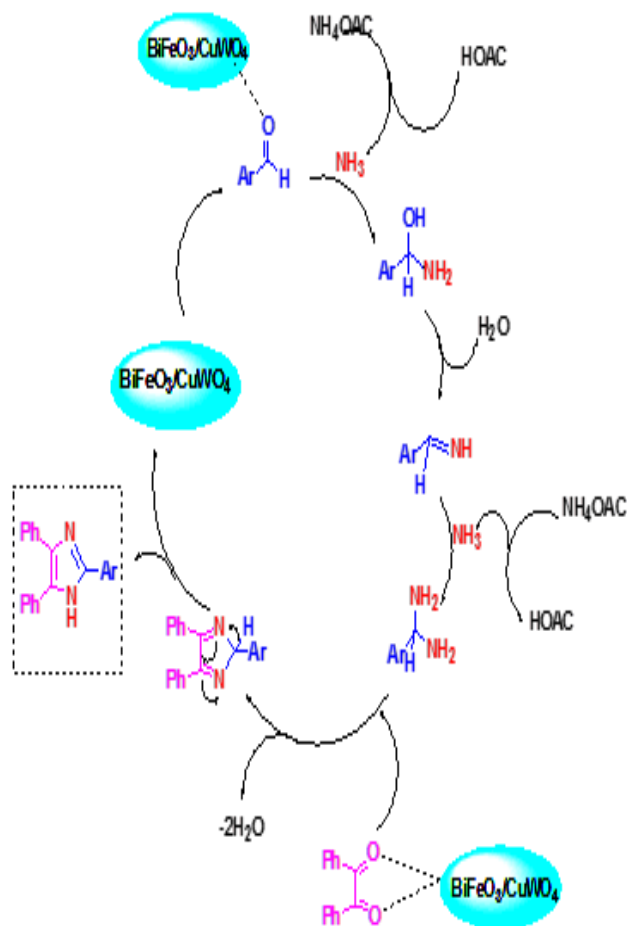
On the one hand, Lower yields which were obtained for electron-donating and ortho substituted aldehydes compared with the electron-withdrawing and para groups may be attributed to the competitive formation of less reactive corresponding imines. On the other hand, electron-withdrawing para derivatives have excellent yields relative to other derivatives, because para derivatives have minimum steric hinderance and electron deficient derivatives can stabilize the

intermediate in comparison to electron rich substituent (Table 2).

A probable mechanistic pathway for the formation of 2,4,5-trisubstituted imidazoles is outlined in Scheme 2. According to the mechanism, it can be proposed that the enormous active centers or unsaturated metal centers in the BiFeO<sub>3</sub>/CuWO<sub>4</sub> heterojunction are responsible for the initial activation of carbonyl group of aldehydes to facilitate nucleophilic addition of ammonia. In more details, it can be proposed that the hydrogen atoms in ammonia and free-orbitals of the metal centers in BiFeO<sub>3</sub>/CuWO<sub>4</sub> that have the lewis acidic properties, are responsible for the activation of carbonyl groups and thus increase the rate of imine production through coordination of the bonding for nucleophilic attack of amines (Scheme 2). It is noteworthy that ammonia itself is produced in situ by decomposition of ammonium acetate in the presence of catalyst. It is considerable that the byproducts of this tandem MCR reaction are mainly water molecules which can be sorbed to the BiFeO<sub>3</sub>/CuWO<sub>4</sub>. Highly catalytic activity of magnetic BiFeO<sub>3</sub>/CuWO<sub>4</sub>

can be attributed to the catalytic temper of metal centers in both of BiFeO<sub>3</sub> and CuWO<sub>4</sub> structure that can easily coordinate with the substrates. We have been compared the catalytic performance of our system with the previously reported results for the

synthesis of 2,4,5-trisubstituted 1H-imidazoles derivatives. The results are summarized in Table 3. Obviously the present protocol is indeed superior to several of the others in terms of product yield, using green solvent-free system, reaction time and catalyst loading.



**Scheme 2.** Plausible mechanism of the reaction

**Table 3.** Catalytic activity comparison of BiFeO<sub>3</sub>/CuWO<sub>4</sub> heterojunction with reported catalysts

Entry	Catalyst	Condition	Time(min)	Yield (%)	Reference
1	Zeolite	EtOH, Reflux	60	80	52
2	Silica sulfuric acid	H <sub>2</sub> O, Reflux	480	81	53
3	Montmorillonite K10	EtOH, Reflux	90	70	52
4	CAN	MeOH, RT	360	75	54
5	NiCl <sub>2</sub> ·6H <sub>2</sub> O/Al <sub>2</sub> O <sub>3</sub>	EtOH/Reflux	90	89	55
6	Co/Ni-MOF	Solvent-free	10	95	56
7	Silica-Choloride	Solvent-free	30	85	57
8	NBS	Solvent-free, 120 °C	45	92	58
9	Yb(OPf) <sub>3</sub>	C <sub>10</sub> /F <sub>18</sub> , 80 °C	360	80	59
10	BiFeO <sub>3</sub> /CuWO <sub>4</sub>	Solvent-free/120 °C	10	98	Present work
11	BiFeO <sub>3</sub>	Solvent-free/120 °C	20	94	Present-work
12	CuWO <sub>4</sub>	Solvent-free/120 °C	24	91	Present-work

An important parameter in heterogeneous catalysis is the reusability of the catalyst. Hence, a set of experiment was carried out to check the reusability of the catalyst for the 2,4,5-trisubstituted-1H-imidazoles synthesis. The magnetic properties of BiFeO<sub>3</sub> aided us for the catalyst separation. The catalyst could be recycled five times without significant loss in its catalytic activity (Figure 8). Decreasing the efficiency of the recycled catalyst is unclear, but may be attributed to the absorption of organic materials on the surface of the catalyst that is not removed during washing with solvents and led to occupy and block the catalytic active sites. As we know, a crucial issue for the solid catalyst is the migration of active sites

from the solid catalyst to the liquid phase. In order to verify the stability of Bi and Fe active sites in BiFeO<sub>3</sub> and Cu and W metals in the CuWO<sub>4</sub> structure a leaching experiment was performed to estimate the contribution of leached active species to the catalytic activity. For this purpose, the reaction was stopped at half of the reaction time (5 min) and the catalyst was completely separated from solution. The remnant of the reaction mixture (without catalyst) was allowed to stir for another period of half the reaction time. As seen in Figure 7, a few amount of 2,4,5-trisubstituted-1H-imidazoles was produced after catalyst separation. After separation of the catalyst the reaction mixture was analysed by AAS technique and no metal was observed.

According to this results negligible under these mild reaction BiFeO<sub>3</sub>/CuWO<sub>4</sub> heterojunction is truly heterogeneous and catalyst leaching is conditions.

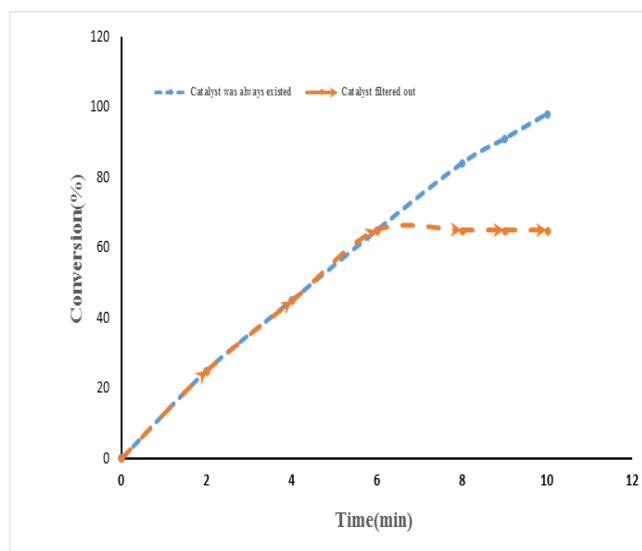


**Figure 7.** The leaching test of BiFeO<sub>3</sub>/CuWO<sub>4</sub> catalyst, before ~ 6 min the two lines are superimposed.

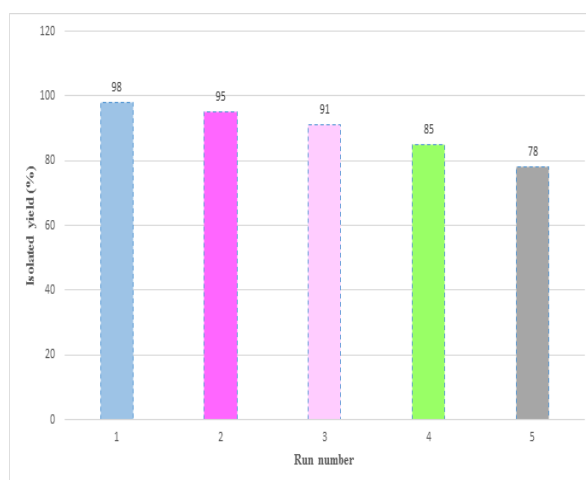


**Figure 8.** Reusability of BiFeO<sub>3</sub>/CuWO<sub>4</sub> catalyst

### Conclusion

In summary, we have introduced a novel BiFeO<sub>3</sub>/CuWO<sub>4</sub> heterojunction structure as a highly effective and recoverable heterogeneous catalyst for the one-pot synthesis of trisubstituted imidazoles under mild solvent free conditions. The high catalytic activity of BiFeO<sub>3</sub>/CuWO<sub>4</sub> is further highlighted when compare to the other catalysts in this reaction. The several advantages of BiFeO<sub>3</sub>/CuWO<sub>4</sub>

as catalyst are easy preparation, recyclability for several times and easiness of separation. In addition to the mild reaction conditions, easy work up, operational simplicity and giving the desired products in good to high yields are the key advantages of this protocol. We have believe that this procedure is appropriate, user-friendly process and economic for the synthesis of substituted imidazoles of biological and medicinal procedure.

### Acknowledgments

I am gratefully acknowledge from the islamic azad university of roodsar branch for financial support of this research.

### References

- [1] N.A. Spaldin, M. Fiebig, *Science*, **2005**, *309*, 391-392.
- [2] W. Eerenstein, N.D. Mathur, J.F. Scott, *Nature*, **2006**, *442*, 759-765.
- [3] M.A. Pena, J.L.G. Fierro, *Chem. Rev.*, **2001**, *101*, 1981-2017.
- [4] H. Tanaka, *Catal. Surv. Asia.*, **2005**, *9*, 63-74.
- [5] F. Gao, X.Y. Chen, K.B. Yin, S. Dong, Z.F. Ren, F. Yuan, T. Yu, Z.G. Zou and J. M. Liu, *Adv. Mater.*, **2007**, *19*, 2889-2892.
- [6] S.M. Sun, W.Z. Wang, L. Zhang and M. Shang, *J. Phys. Chem. C.*, **2009**, *113*, 12826-12831.
- [7] Y.N. Huo, M. Miao, Y. Zhang, J. Zhu, H.X. Li, *Chem. Commun.*, **2011**, *47*, 2089-2091.
- [8] Z.X. Li, Y. Shen, C. Yang, Y.C. Lei, Y.H. Guan, Y.H. Lin, D.B. Liu and C.W. Nan, *J. Mater. Chem. A.*, **2013**, *1*, 823-829.
- [9] Z.X. Li, Y. Shen, Y.H. Guan, Y.B. Hu, Y.H. Lin and C.W. Nan, *J. Mater. Chem. A.*, **2014**, *2*, 1967-1973.
- [10] J.F. Dai, T. Xian, L.J. Di, H. Yang, *J. Nanomater.*, **2013**, *2013*, 1-5.
- [11] S. Shetty, V.R. Palkar, R. Pinto, *Pramana J. Phys.*, **2002**, *58*, 1027-1030.
- [12] J.K. Kim, S.S. Kim, W.J. Kim, *Mater. Lett.*, **2005**, *59*, 4006-4009.
- [13] Z.C. Quan, H. Hu, S. Xu, W. Liu, G.J. Fang, M.Y. Li, X.Z. Zhao, *J. Sol-Gel Sci. Technol.*, **2008**, *48*, 261-266.
- [14] J.H. Luo, P.A. Maggard, *Adv. Mater.*, **2006**, *18*, 514-517.
- [15] C. Chen, J. Cheng, S. Yu, L.J. Che, Z.Y. Meng, *J. Cryst. Growth.*, **2006**, *291*, 135-139.
- [16] G.D. Achenbach, W.J. James, R. Gerson, *J. Am. Ceram. Soc.*, **1967**, *8*, 437-438.
- [17] M. Valant, A.K. Axelsson, N. Alford, *Chem. Mater.*, **2007**, *19*, 5431-5436
- [18] S. Farhadi, N. Rashidi, *Polyhedron*, **2010**, *29*, 2959-2965.
- [19] C.M. Cho, J.H. Noh, I. Cho, J. An, K.S. Hong, *J. Am. Ceram. Soc.*, **2008**, *91*, 3753-3755.
- [20] M.A. Ahmeda, N. Okashab, S.F. Mansourc, S.I. El-deka, *J. Alloys Compd.*, **2010**, 345-350.
- [21] V.B. Mikhailik, H. Kraus, *J. Phys. D Appl. Phys.*, **2006**, *39*, 1181.
- [22] S.K. Arora, T. Mathew, B. Chudasama and A. Kothuri, *J. Cry. Grow.*, **2005**, *1*, 651-656.
- [23] O.Y. Khyzhun, V.L. Bekenev, Y. Solonin, *J. Alloy, Compd.*, **2009**, *2*, 184-189.
- [24] A. D'omling, W. Wang and K. Wang, *Chem. Rev.*, **2012**, *6*, 3083-3135.
- [25] Kumar D, Kommi DN, Bollineni N, Patel AR, Chakraborti AK, *Green Chem.*, **2012**, *7*, 2038-2049.
- [26] V.S.V. Satyanarayana, A. Sivakumar, *Chem. Pap.*, **2011**, *4*, 519-526.
- [27] M. Antolini, A. Bozzoli, C. Ghiron, G. Kennedy, T. Rossi, A., *Bioorg. Med. Chem. Lett.*, **1999**, *7*, 1023-1028.
- [28] L. Wang, K.W. Woods, Q. Li, K.J. Barr, R.W. McCroskey, S.M. Hannick, L. Gherke, R.B. Credo, Y.H. Hui, K. Marsh, R. Warner, J.Y. Lee, N.Z. Mozng, D. Frost, S.H. Rosenberg, H.L. Sham, Potent, *J. Med. Chem.*, **2002**, *8*, 1697-1711.
- [29] A.K. Takle, M.J.B. Brown, S. Davies, D.K. Dean, G. Francis, A. Gaiba, A.W. Hird, F.D. King, P.J. Lovell, A. Naylor, A.D. Reith, J.G. Steadman, D.M. Wilson, *Bioorg. Med. Chem. Lett.*, **2006**, *2*, 378-381.



- [30] J. Heeres, L.J.J. Backx, J.H. Mostmans, J. Van Custem, *J. Med. Chem.*, **1979**, 8, 1003–1005.
- [31] J.C. Lee, J.T. Laydon, P.C. McDonnell, T.F. Gallagher, S. Kumar, D. Green, D. McNulty, M.J. Blumenthal, J.R. Keys, S.W.L. Vatter, J.E. Strickler, M.M. McLaughlin, I.R. Siemens, S.M. Fisher, G.P. Livi, J.R. White, J.L. Adams, P.R. Young, *Nature*, **1994**, 739–746.
- [32] R. Schmierer, H. Mildenerger, H. Buerstell, German Patent 361464, **1987**, *Chem. Abstr.*, 1988, 108, 37838.
- [33] E. Cavusoglu, J. E. Freedman, J. Loscalzo, *New. Thera. Agent. Thrombos. Thrombolys.*, **2009**, 67-98.
- [34] A.R. Khosropour, *Ultrason. Sonochem.*, **2008**, 5, 659-664.
- [35] L.M., Wang, Y.H., Wang, H. Tian, Y.F., Yao, J.H., Shao, B. Liu, *J. Fluorine. Chem.*, **2006**, 12, 1570-1573.
- [36] M. Xia, Y.D. Lu, *J. Mol. Catal. A: Chem.*, **2007**, 1, 205-208.
- [37] M.V. Chary, N.C. Keerthysri, S.V. Vupallapati, N. Lingaiah, S. Kantevari, *Catal Commun.*, **2008**, 10, 2013-2017.
- [38] J. Safari, S.D. Khalili, S.H. Banitaba, H. Dehghani, *J. Korean Chem. Soc.*, **2011**, 55, 1–7.
- [39] W. Luo, L.H. Zhu, N. Wang, H.Q. Tang, M.J. Cao, Y.B. She, *Environ. Sci. Technol.*, **2010**, 44, 1786–1791.
- [40] W. Luo, L. Zhu, N. Wang, H. Tang, M. Cao, Y. She, *Environ. Sci. Technol.*, **2010**, 5, 1786-1791.
- [41] M. Kidwai, P. Mothsra, V. Bansal, R.K. Somvanshi, A.S. Ethayathulla, S. Dey, T.P. Singh, *J. Mol. Catal. A: Chem.*, **2007**, 265(1), 177-182.
- [42] I. Lantos, W. Y. Zhang, X. Shui, D.S. Eggleston, *J. Org. Chem.*, **1993**, 25, 7092-7095.
- [43] J. Safari, Sh. Dehghan Khalili, S.H. Banitaba, *J. Chem. Sci.*, **2010**, 3, 437-441.
- [44] T.D.A. Kumar, N. Yamini, C. Subrahmanyam, K. Satyanarayana, *Synth. Commun.*, **2014**, 15, 2256-2268.
- [45] S.E. Wolkenberg, D.D. Wisnoski, W.H. Leister, Y. Wang, Z. Zhao, C. W. Lindsley, *Org. Lett.*, **2004**, 9, 1453-1456.
- [46] K. Nikoofar, M. Haghghi, M. Lashanizadegan, Z. Ahmadvand, *J. Taibah. Uni. Sci.*, **2015**, 4, 570-578.
- [47] S. Samai, G.C. Nandi, P. Singh, M.S. Singh, *Tetrahedron*, **2009**, 49, 10155-10161.
- [48] B.F. Mirjalili, A. Bamoniri, M.A. Mirhoseini, *Sci. Iran. C.*, **2013**, 3, 587-591.
- [49] H.R. Shaterian, M. Ranjbar, K. Azizi, *J. Iran. Chem. Soc.*, **2011**, 4, 1120-1134.
- [50] J. Safari, S.D. Khalili, M. Rezaei, S.H. Banitab, F. Meshkani, *Monatsh. Chem.*, **2010**, 141, 1339–1345.
- [51] G.H. Mahdavinia, A.M. Amani, H. Sepehrian, *Chin. J. Chem.*, **2012**, 3, 703-708.
- [52] D.M. White, J. Sonnenberg, *J. Org. Chem.*, **1964**, 7, 1926-1930.
- [53] A. Teimouri, A.N. Chermahini, *J. Mol. Catal. A: Chem.*, **2011**, 1, 39-45.
- [54] A. Shaabani, A. Rahmati, *J. Mol. Catal. A: Chem.*, **2006**, 1, 246-148.
- [55] A. Shaabani, A. Maleki, M. Behnam, *Synth. Commun.*, **2009**, 1, 102–110.
- [56] M.M. Heravi, K. Bakhtiari, H.A. Oskooie, S. Taheri, *J. Mol. Catal. A: Chem.*, **2007**, 1, 279-281.
- [57] H. Ramezanalizadeh, F. Manteghi, *Monatshefte*, **2016**, DOI: 10.1007/s00706-016-1776-9.
- [58] H.V. Chavan, D.K. Narale, *C. R. Chim.*, **2014**, 10, 980-984.
- [59] B. Maleki, S.S. Ashrafi, *J. Mex. Chem. Soc.*, **2014**, 1, 76-81.
- [60] M.G. Shen, C. Cai, W.B. Yi, *J. Fluorine. Chem.*, **2008**, 6, 541-544.